IGSHPA Research Track
Las Vegas, December 6-8, 2022

Column Experiments to Anticipate Clogging of Standing Column Wells

Léo Cerclet **Benoît Courcelles** **Philippe Pasquier**

ABSTRACT

Standing column wells are a promising solution to reduce the environmental footprint of building energy consumption. Nevertheless, as in other open-loop wells, they can be affected by clogging processes if detrimental hydrogeological conditions are present locally. This problem is relatively rare and still difficult to anticipate, even though some specific factors have been reported, such as substratum mineralogy and groundwater quality. This study proposes the use of a column experiments and coupon cell to anticipate clogging at two different sites near Montréal, Canada. The experiments were performed for duration of 50 and 52 d using thermoregulated columns at four temperatures. The results identified a difference in the chemistry of each site without any significant clogging risk. Site A showed a decrease in carbonates, magnesium, and calcium ions, and scanning electron microscopy showed a minor tendency to form carbonate deposits. Sulfate and calcium dissolution of the bedrock material were observed at Site B. Scanning electron microscopy of the coupons revealed organic matter with high carbon and sulfate concentrations. The same type of deposits was observed at Site B after three years of operation. In conclusion, these tests helped identify various potential clogging phenomena and indicated that both sites are not susceptible to major clogging risks.

INTRODUCTION

Ground-source heat pumps have demonstrated their ability to reduce the environmental footprint of building energy consumption. As has been demonstrated, owing to their original design, standing column wells (SCW) incur lower costs and have a higher thermal efficiency than traditional closed-loop configurations (O'Neill et al., 2006; Pasquier et al., 2016). The SCW is a coaxial uncased well in which groundwater constitutes the heat-carrier fluid. A major portion of the groundwater is recycled inside the SCW. Occasionally, some of the groundwater can be discharged outside the main well to force a converging flow towards the SCW (Pasquier et al., 2016). As with other open-loop systems, SCW can be affected by clogging processes if detrimental conditions are locally present. Although relatively rare in practice and with varying degrees of severity, this issue is well known to hydrogeologists. The main problem with clogging is that it is still difficult to anticipate, even though it has been reported that specific factors influence these processes, such as substratum mineralogy, groundwater quality, design, and geothermal operation. The main operations that favor scaling are the cooling period and the presence of CO_2 degasification (Eppner et al., 2017). The bleeding operation is beneficial to chemical stability as it allows the minimization of the impact of temperature modification (Eppner et al., 2017).

A promising strategy for anticipating clogging is to perform a laboratory column experiment to reproduce these factors. In open-loop systems, clogging can be observed in underground and aboveground equipment (Gjengedal et al., 2019). Kim et al. (2017) identified biological clogging in the underground equipment of an SCW, and Cerclet et al. (2020) observed minor calcite scaling on the aboveground equipment. A strategy to understand clogging processes involves carrying out column experiments. This method has multiple advantages, as demonstrated by the following two studies. For instance, Griffioen and Appelo (1993) performed a column experiment at a fixed temperature of 90 °C and identified calcite precipitation. In addition, this experiment highlighted the necessity of using native sediments and

Léo Cerclet (leo.cerclet@polymtl.ca) is a PhD student, Department of Civil, Geological and Mining Engineering, Polytechnique Montréal
Benoît Courcelles (benoit.courcelles@polymtl.ca) is a professor of civil engineering at Polytechnique Montréal
Philippe Pasquier (philippe.pasquier@polymtl.ca) is a professor of geological engineering at Polytechnique Montréal.

DOI: https://doi.org/10.22488/okstate.22.000023

groundwater to anticipate the kinetic precipitation of natural systems. Rinck-Pfeiffer et al. (2000) demonstrated that column experiments have the advantage of identifying the interrelationships between the physical, biological, and chemical clogging processes. To help anticipate clogging at the design stage of an SCW system, we propose the use of a column experiment along with coupons made of copper and stainless steel to consider both temperature changes and the material of aboveground equipment.

COLUMN EXPERIMENTS

Column experiments were designed to identify clogging processes linked to SCW operation. As clogging can occur on underground and aboveground equipment, the experiment is composed of two parts, described below. Two sites were investigated in this study. Groundwater and drill cuttings from each site were collected and used to construct a column.

Column Construction

A schematic representation of the column experiment is shown in Figure 1. The large rectangle in Figure 1 (a) and photograph in Figure 1 (c) represent the underground SCW. It is composed of a column filled with drill cuttings and saturated with groundwater sampled from the SCWs. The relative density and soil distribution were measured to characterize drill cutting. Groundwater was injected at the bottom of the column at an initial flow rate of 0.012 L/min. A low flow was selected to maximize contact between the groundwater and drill cuttings. The internal column was 20.0 cm in diameter and 51.8 cm in height. Three pressure sensors were placed 22.25, 32.25, and 39.45 cm from the bottom. The maximum pressure in a real SCW corresponds typically to the water column height. This high pressure could not be reproduced using column experiment equipment. Note that the maximum pressure recorded by the sensors was 5.99 kPa and 6.05 kPa, respectively in Columns A and B. To avoid vacuum pressure in the column, the top was opened to the atmosphere allowing the gases dissolved to be equilibrated with the atmosphere. Consequently, the gases dissolved in groundwater can be equilibrated with the atmosphere. This situation is the worst for the scaling process (Eppner et al., 2017). A multiparameter probe for pH, ORP, temperature, and specific conductivity was placed at the exit from where the samples were collected. The equipment was calibrated every week. The cooling period is the most damaging for geothermal equipment (Eppner et al., 2017). Thus, a heating period of 4 °C was imposed as a conditioning period, followed by two cooling periods of 25 and 35 °C. The temperature was initially maintained for 14 days. The batch tests (not shown) concluded that it was sufficient to reach equilibrium with a lower surface-to-volume ratio. However, a period of seven days at a temperature of 20 °C was added to minimize the impact of a power breakdown that was initially planned in the building but did not occur. Subsequently, the same protocol was applied to both columns. Four different temperature conditions (4, 20, 25, and 35 °C) were imposed on the 25-liter groundwater reservoir, column, and multiparameter cell. The groundwater reservoir was immersed in a temperature-controlled cooling and heating bath. A cooling/heating circuit was wound around the column, and a multiparameter cell was used to prevent heat loss or gain. In addition, the column and multiparameters were insulated with a mineral wool layer and an aluminum layer. The tubes coming from or leaving the controller were also insulated.

The outlet groundwater was sent to a cell containing two coupons. This cell represents the aboveground part of a geothermal system. The coupons were composed of standard microscope slides made of copper and stainless steel. These materials were chosen because they are locally used in HVAC applications. At the end of the tests, coupon surfaces were analyzed using scanning electron microscopy (SEM) to identify any deposits. Finally, groundwater was collected in a thermoregulated reservoir and reinjected into the column. This experiment could reproduce a standing column that operates well under full recirculation mode.

Column Experiments

For each column, the experiment was performed for 50 and 52 d, and 36 and 38 samples were collected and filtered, respectively for Columns A and B. The major anions and cations were analyzed by ion chromatography. Alkalinity was measured using an automatic titrator from Hanna. These results were used to calculate the saturation index (SI) of each sample. The saturation index was calculated using the following equation:

$$SI = \log\left(\frac{IAP}{K_{sp}}\right) \quad (1)$$

where IAP is the ion activity product and K_{sp} is the solubility product.

The SI value indicates the saturation state of each mineral. If SI > 0, it is supersaturated, leading to precipitation. In contrast, if SI < 0, it is undersaturated, which leads to dissolution. This calculation was performed using the PHREEQC software on the database, wateq4f (Parkhurst and Appelo, 2013). At each site, drill cuttings and groundwater were collected to fill the columns. Groundwater was collected 48 h before the start of the experiment, was not filtered and was cooled during the 1- or 2-hour transport. The samples were stored in a cold chamber at 6 °C. Even if the reservoir was closed, degassing of the groundwater could have occurred before the column experiment started.

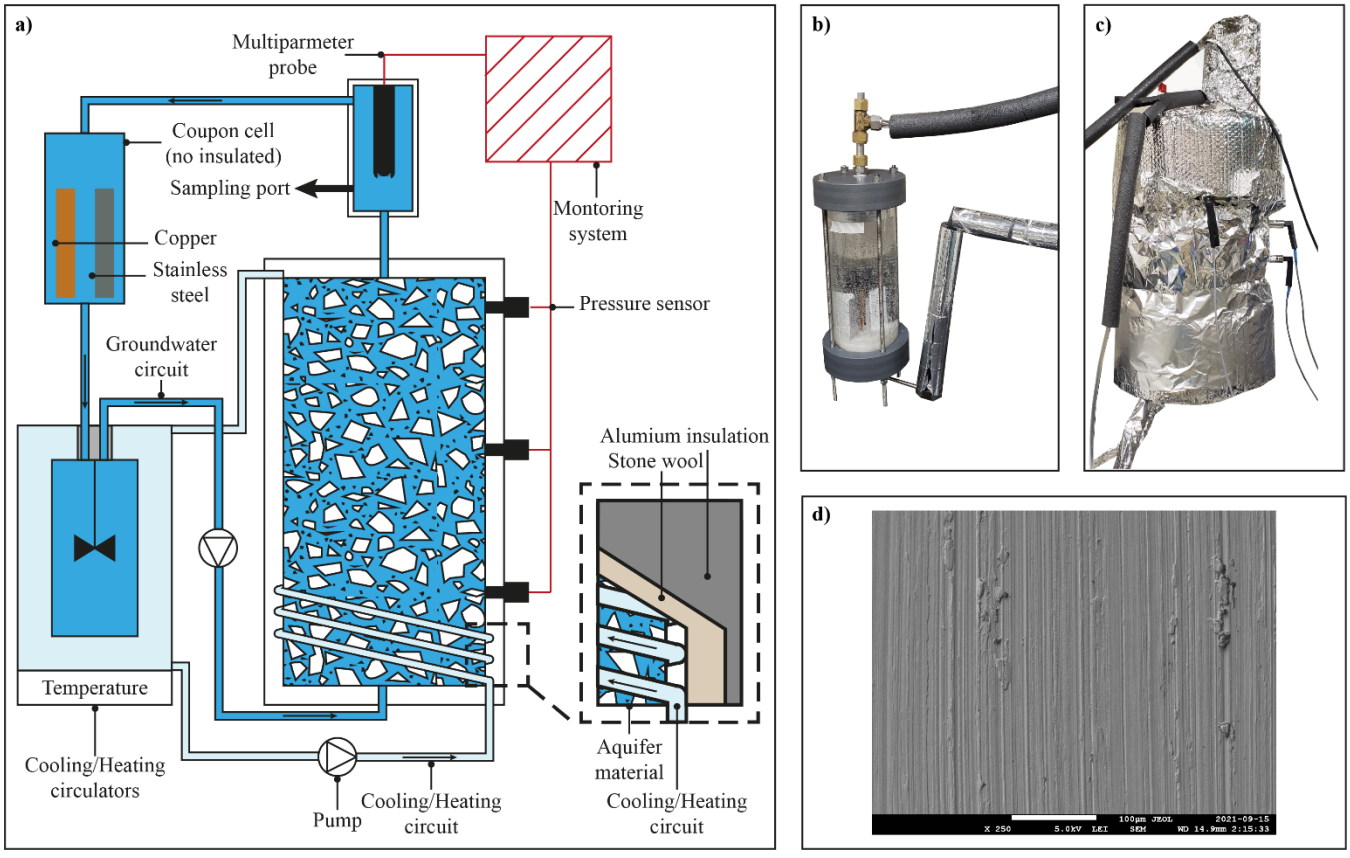

Figure 1 a) Schematic representation of the column experiments, the inset shows the spiral coil and two layers of insulation, b) coupon cell, c) experimental column and the multiparameter cell d) the microscope results for stainless steel before the experiment at a large focus x250.

Site A corresponded to the site presented by Robert et al. (2022). The bedrock is mainly composed of dolomite and quartz arenite. The main dimensions are 133.2 m in depth and 0.159 m in diameter. The initial groundwater temperature was 8.7 °C. The SCWs at Site A have only recently been commissioned. Site B corresponded to the site presented by

Beaudry et al. (2019). The bedrock is mostly composed of gray mudstone, siltstone, sandstone, and limestone. The main dimensions are a depth of 215 m and a diameter of 0.165 m. The initial groundwater temperature was 11.0 °C. This site has the advantage of being operated intermittently and has been studied since 2016. The chemical characteristics of the bedrock are presented in Table 1. The bedrock of Site A has more calcium and magnesium than that of Site B. Conversely, the bedrock of Site B has a greater concentration of sulfate and iron than Site A. As Site A has a loss on ignition (LOI) equal to its CO_2 content, all carbon seems to be in this form.

RESULTS AND DISCUSSION

This section presents the chemical analysis performed on Columns A and B, which are representative of Sites A and B, respectively. These analyses were performed using the results from the SEM of coupons to evaluate their impact on the aboveground equipment. The pressure records did not show significant pressure modifications during the 50- or 52-day column experiments. The hydraulic conductivity of Column A remained constant, whereas the hydraulic conductivity of Column B increased from $7.3.10^{-7}$ m/s to $8.1.10^{-7}$ m/s. An explanation for this slight change could be that the 25-liter reservoir did not bring enough contamination to clog columns A and B with porosities of 0.21 and 0.32. Nevertheless, this volume was chosen to achieve equilibrium between the rock and water in a short period of time. Indeed, the ratios of the rock surface to the water volume are 144 and 119 times higher than those of their real SCW, respectively, for Columns A and B. The ratio is an approximation that considers the cuttings as spherical and the SCW borehole as a smooth cylinder. This column test with recirculation is still representative of an SCW that is operated without bleeding. During this operation, a significant volume of water was recirculated inside the uncased well. The hypothesis was that equilibrium between the borehole and groundwater was achieved. Note that for temperatures of 4 °C and 35 °C, the insulation was not sufficient to keep the temperature constant across the bottom and the top of the column. The temperatures of the outlets were maintained at 8 °C and 32 °C.

Table 1. Geochemical and hydraulic characteristics of column experiment.

	Site A	Site B
Chemical formula (%)		
Al_2O_3	3.42	14.02
CaO	12.97	7.79
MgO	8.76	3.02
Fe_2O_3	1.20	6.62
Na_2O	0.06	1.05
K_2O	1.90	2.79
MnO	0.11	0.06
SO_3	1.40	2.63
CO_2	20.51	7.11
LOI	20.43	10.99
$Carbon\ (total)$	5.64	2.94
Hydraulics		
Porosity	0.21	0.32
Drill cutting mass (kg)	33.95	28.18
Relative density	2.76	2.71

Piper Diagram

The Piper diagram represents the concentration percentages of the major anions and cations. Figure 2 shows results of the samples collected in Columns A (36 samples) and B (38 samples). Note that 11 analyses for Column A have an electric balance of 5–10 %. All other analyses had electric balances of less than 5 %, indicating good chemical analyses. The two columns have different chemical compositions: The chemical composition of Column A has a repartition of approximately 30 % calcium / 70 % magnesium, whereas that of Column B corresponds to sulfated groundwater. However, the relative changes were not significant. Site A has been more exposed to calcium or magnesium carbonate

precipitation because of its chemistry. Site B has groundwater that mainly contains sulfates and bedrock with organic carbon and iron. Thus, this site has been more exposed to biochemical clogging. Indeed, calcite precipitation is generally slower than biological clogging for the range of temperatures tested. Therefore, Site B could be impacted in a shorter time frame than Site A. Because the chemical behaviors of these two sites were different, they were analyzed separately.

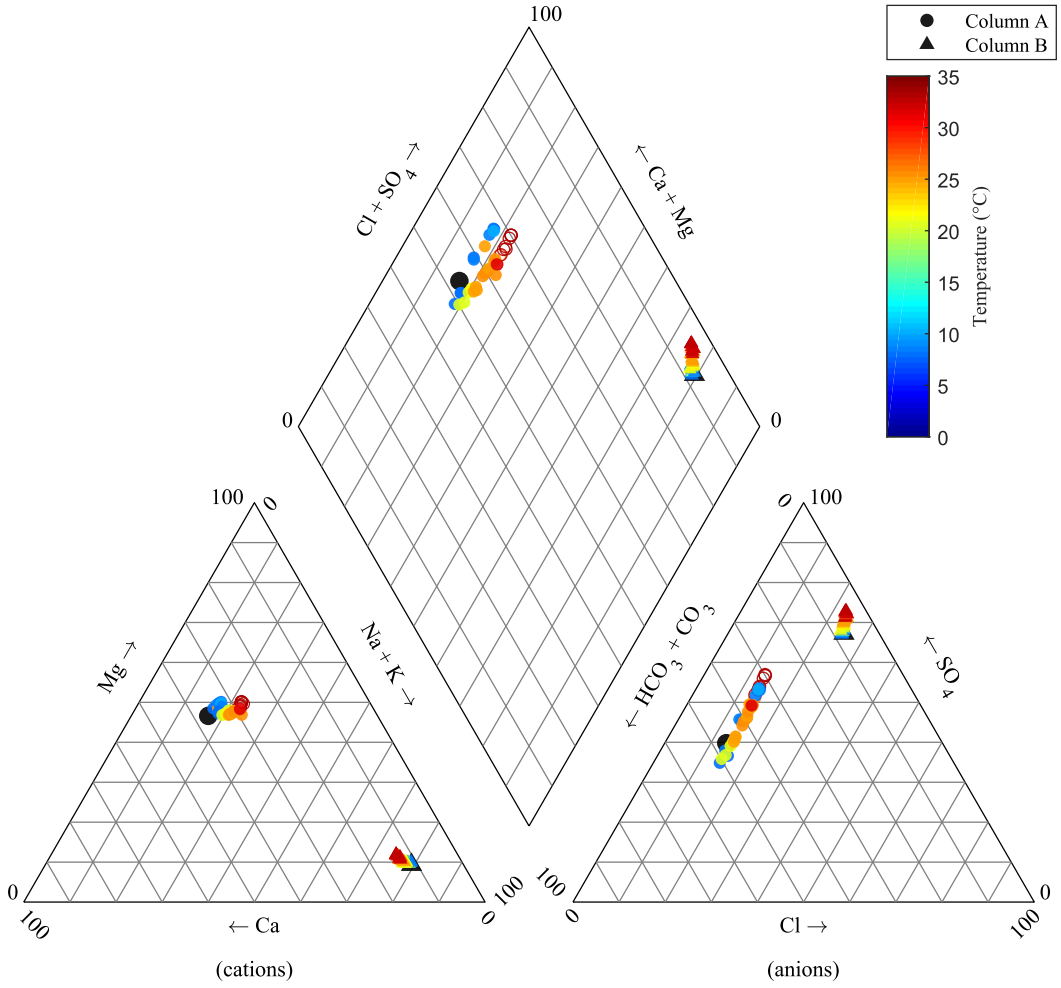

Figure 2 Piper diagram presenting the results for both column experiments. Empty bullet point corresponds to the analyses with electric balances greater than 5 %; the large black marker corresponds to the initial state.

Column A

Figure 3 shows the evolution of calcium, magnesium, and bicarbonate concentrations as a function temperature, and time. This figure shows a decrease in magnesium, calcium, and bicarbonate concentrations with increasing temperature and duration. This decrease is attributed to precipitation of calcite ($CaCO_3$) or dolomite ($CaMg(CO_3)_2$), as their saturation indexes (SI) remain greater than zero. The magnesite ($MgCO_3$) SI remained below zero, and the mineral remained dissolved. Owing to the decrease in magnesium concentration, dolomite precipitation is dominant in comparison to magnesite dissolution.

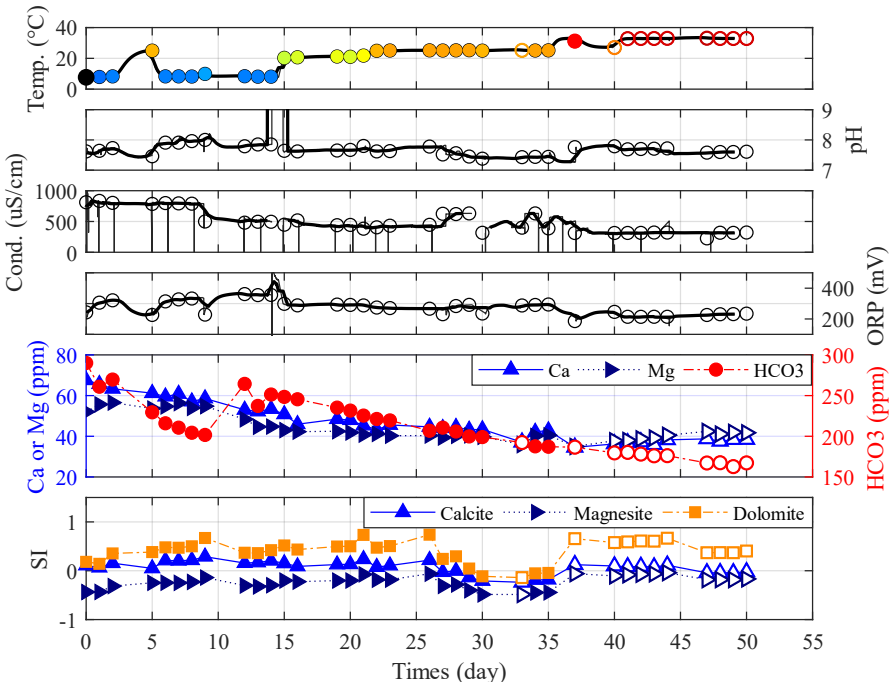

Figure 3 Physicochemical parameters and the carbonate precipitation for Column A as a function of time; empty marker corresponds to the sample with an electric balance of above 5 %.

Figure 4 shows the microscopic analysis of the stainless-steel coupons of Column A. The microscopic analysis in Figure 4 (a) shows minor roughness. In fact, some depositions were observed only with a close focus. The deposition of the stainless-steel coupons was analyzed using SEM, as shown in Figure 4 (b). SEM analysis corresponds to the observations in Figure 3 and is representative of a dolomite ($CaMg(CO_3)_2$) or magnesium-calcite ($CaMgCO_3$) deposit. Note that microscopic analysis of the copper coupon is not presented because the deposition was superficial and resulted mainly in oxidation. In conclusion, the column experiment at this site allowed for the identification of the principal cause of potential clogging, which is carbonate precipitation. Nevertheless, the weak rate of deposition on the coupon and weak hydraulic conductivity evolution in the column allowed us to consider this site as not at risk for clogging in the recirculation mode. The reservoir volume could have limited the deposits.

a) b)

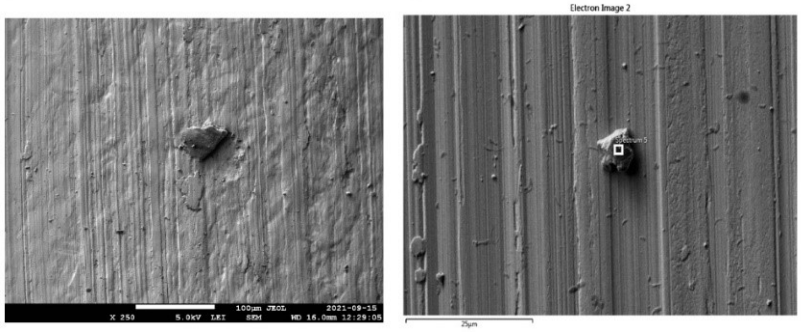

	At%
O	53.5
C	19.6
Ca	11.6
Mg	10.8
Fe	2.6
Si	1.1
S	0.5
Al	0.3

Figure 4 Microscope results for stainless steel in Column A. a) large focus at x250, b) close focus at x2500.

Column B

Figure 5 shows the evolution of magnesium, calcium, bicarbonate, and sulfate concentrations as a function of temperature, and time for Site B. The first observation is that the water surrounding Column B is more mineralized than that surrounding Column A. Thus, the site is naturally more exposed to clogging issues. The sulfate and calcium concentrations in Column B increased with temperature and time. The saturation indexes of gypsum ($CaSO_4$ $2H_2O$) (not represented) and anhydrite ($CaSO_4$) remain below zero. Thus, the increase in calcium concentration seems to be related to the dissolution of gypsum or anhydrite. This concentration increase can eventually cause calcite ($CaCO_3$) precipitation, as shown in Figure 5. Calcite precipitation causes a decrease in bicarbonate concentration, which leads to the dissolution of dolomite or magnesite and an increase in magnesium concentration. Finally, the dissolution of gypsum can lead to dedolomitization (Appelo and Postma, 2004).

Note that iron concentrations were not analyzed in the groundwater. However, analyses indicated 6.62 % of iron oxides in the rock samples analyzed. The presence of pyrite (FeS_2) is then deemed likely in this geological context. The groundwater circuit is not isolated from the atmosphere. Therefore, groundwater recirculation can oxidize pyrite, which can lead to an increase in sulfate concentration and acidity. This acidity can neutralize alkalinity due to CO_3 and HCO_3. In conclusion, the main geochemical process in the SCW is mineral dissolution, which can explain the small hydraulic conductivity change.

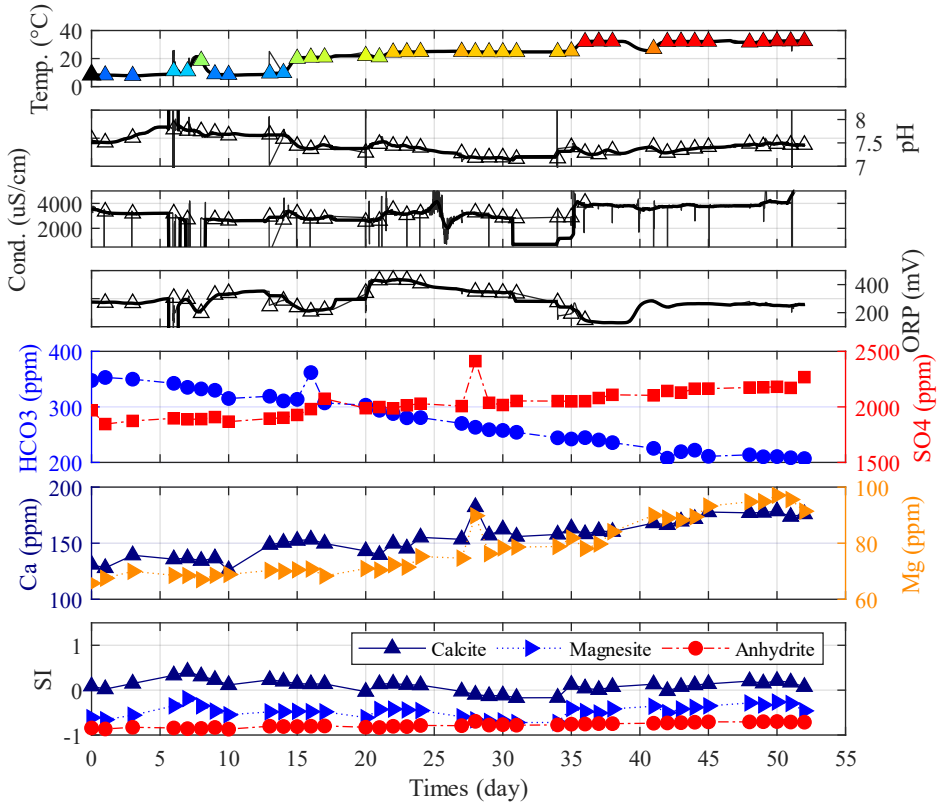

Figure 5 Physicochemical parameters and dissolution of anhydrite and diminution in carbonates for Column B as functions of time.

Another observation is that the deposition on coupons in Column B is more important than that in Column A, as shown in Figure 6 (a). This means that Site B is more exposed to clogging in the aboveground equipment. The deposits in Figure 6 (b) are likely to be organic matter composed of carbon, oxygen, iron, and sulfur (spectrum 3). Notably, iron concentration could be overestimated. Indeed, the analyses could have considered a part of the stainless-steel support

owing to the porosity of the organic matrix. The presence of an organic matrix is in accordance with the geochemistry of this site, which contains more organic carbon (Table 1). Inside the organic deposits, some salts, such as chloride or sodium, were identified (spectra 2 and 4). These results demonstrate the synergy between mineral precipitation and microbial growth. Note that calcium concentration could not be analyzed because of the proximity of carbon and oxygen peaks. This did not exclude the occurrence of calcite precipitation. As in Site A, the copper coupon had less deposition than the stainless-steel coupon. The main roughness observed was due to copper oxidation.

At Site B, the dissolution of the reactive bedrock with sulfur, iron, and carbon favors biochemical deposition in the aboveground equipment, and this deposition was only observed with a microscope. The column test did not reveal any significant clogging at this site. Indeed, the SCW has been operating at this site since 2016 and has not suffered from any major clogging. Minor depositions were observed twice using an optical flowmeter during routine verification. The first deposition was composed of calcite and was observed in January 2019 (Cerclet et al., 2020). The second deposition was observed in July 2019. These observations are illustrated in Figure 6. The deposits were mainly composed of carbon, sulfur, and iron. In conclusion, the column experiment identified two potential processes of deposition and their locations in the ground source heat pump system. These results, obtained in 52 days, correspond to the observations made at Site B after three years of operation. Thus, this column experiment had the ability to anticipate the scaling of aboveground equipment even though this site and the column did not suffer from any significant clogging.

a)

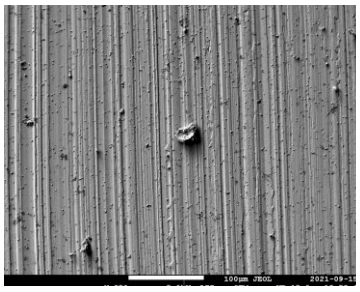

b)

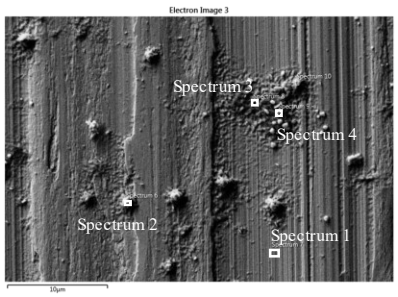

	Spectrum 1 At%	Spectrum 2 At%	Spectrum 3 At%	Spectrum 4 At%	July 2019 (n=14) At%
Fe	66.0	3.2	24.3	3.1	4.2
Cr	18.1	0.0	0.0	0.0	-
Ni	9.0	0.0	0.0	0.0	-
C	3.6	33.6	18.7	39.2	20.5
O	2.6	31.4	18.3	33.2	28.0
Si	0.7	3.2	3.0	3.9	5.7
Na		11.9	3.2	5.9	1.5
S		4.5	4.3	4.2	5.3
Cl		3.3	0.8	2.3	0.5
Ca		2.9	2.9	2.9	0.8
Mg		2.6	1.8	2.3	0.7

Figure 6 Microscope results for the stainless steel in Column B. a) large focus at x250. b) present scanning electron close focus at x2500 (red values are the highest imported concentration, green values are estimated). The column of July 2019 presents the mean results of the analysis performed on a deposit collected from Site A after 3 years of standing column well operation.

CONCLUSION

This study presented a protocol relying on a column experiment and coupons to predict clogging in SCW installations with temperature regulation and groundwater recirculation. The feedback from the operation of the two columns demonstrated that this experiment was appropriately designed to identify the main deposition processes. The small deposits observed in Column B after 52 days corresponds to the observation at Site B after three years of operation. In addition, these experiments highlighted the differences between the two sites under similar operating conditions. Experimental results indicate that Site B is more susceptible to biochemical clogging due to organic carbon and sulfates, whereas Site A is more sensitive to carbonate precipitation. However, the results and analyses indicate that neither site is prone to significant clogging risks. The limitations of our study were the possibility that the dissolved groundwater gases were modified before the column started. Further work is required to analyze a clogging site for evaluating underground equipment.

ACKNOWLEDGMENTS

The authors wish to acknowledge the support and funding provided by the Natural Sciences and Engineering Research Council of Canada (grant number RDCPJ 530945), Hydro-Québec, FTE drilling, Marmott Energies and Richelieu Hydrogeology.

REFERENCES

Appelo, C.A.J., Postma, D., 2004. *Geochemistry, groundwater and pollution*. CRC press.

Beaudry, G., Pasquier, P., Marcotte, D., 2019. *The impact of rock fracturing and pump intake location on the thermal recovery of a standing column well: model development, experimental validation, and numerical analysis*. Science and Technology for the Built Environment 25, 1052–1068. https://doi.org/10.1080/23744731.2019.1648133

Cerclet, L., Courcelles, B., Pasquier, P., 2020. *Impact of Standing Column Well Operation on Carbonate Scaling.* Water 12, 2222. https://doi.org/10.3390/w12082222

Eppner, F., Pasquier, P., Baudron, P., 2017. *A coupled thermo-hydro-geochemical model for standing column well subject to CO2 degassing and installed in fractured calcareous aquifers*. Geomechanics for Energy and the Environment 11, 14–27. https://doi.org/10.1016/j.gete.2017.05.003

Gjengedal, S., Ramstad, R.K., Hilmo, B.O., Frengstad, B.S., 2019. *Fouling and clogging surveillance in open loop GSHP systems*.

Kim, H., Mok, J.-K., Park, Y., Kaown, D., Lee, K.-K., 2017. *Composition of groundwater bacterial communities before and after air surging in a groundwater heat pump system according to a pyrosequencing assay*. Water 9, 891.

O'Neill, Z.D., Spitler, J.D., Rees, S., 2006. *Performance analysis of standing column well ground heat exchanger systems*. ASHRAE

Parkhurst, D.L., Appelo, C.A.J., 2013. *Description of input and examples for PHREEQC version 3: a computer program for speciation, batch-reaction, one-dimensional transport, and inverse geochemical calculations* (USGS Numbered Series No. 6-A43), Techniques and Methods. U.S. Geological Survey, Reston, VA.

Pasquier, P., Nguyen, A., Eppner, F., Marcotte, D., Baudron, P., 2016. *Standing column wells. Advances in Ground-Source Heat Pump Systems* 269–294.

Rinck-Pfeiffer, S., Ragusa, S., Sztajnbok, P., Vandevelde, T., 2000. *Interrelationships between biological, chemical, and physical processes as an analog to clogging in aquifer storage and recovery (ASR) wells.* Water Research 34, 2110–2118.

Robert, S., Pasquier, P., Nguyen, A., 2022. *Impact of layered heterogeneity on thermal response test interpretation performed on a standing column well operated without bleed.* Geothermics 101, 102353. https://doi.org/10.1016/j.geothermics.2022.102353